1 **Environmental cholera (*Vibrio cholerae)* dynamics in an estuarine system in southern**

2 **coastal Ecuador**

3

4 *RH: Dynamics of Vibrio cholerae in southern Ecuador*

5

6 Sadie J. Ryan*[1,2]*,* Anna M. Stewart Ibarra[3], Eunice Ordóñez[4], Winnie Chu[5], Julia L. Finkelstein[5],

7 Christine A. King[6], Luis E. Escobar[3,7], Christina Lupone[3], Froilan Heras[3], Erica Tauzer[3], Egan

8 Waggoner[3], Tyler G. James[1,2], Washington B. Cárdenas[4], Mark Polhemus[3]

9 *Corresponding author: sjryan@ufl.edu, (352) 294-7513

10 1. Department of Geography and Emerging Pathogens Institute. University of Florida,

11   Gainesville, FL, USA.

12 2. Emerging Pathogens Institute. University of Florida, Gainesville, FL, USA.

13 3. Center for Global Health and Translational Science, SUNY Upstate Medical University,

14   Syracuse, NY, USA.

15 4. Laboratorio de Biomedicina, FCV, Escuela Superior Politécnica del Litoral, Guayaquil,

16   Ecuador.

17 5. Division of Nutritional Sciences, Cornell University, Ithaca NY, USA

18 6. Department of Microbiology and Immunology, SUNY Upstate Medical University,

19   Syracuse, NY, USA.

20 7. Department of Fisheries, Wildlife, and Conservation Biology, University of Minnesota, Saint

21   Paul, MN, USA.

22

24   **Word count:** 3616

25

26   **Acknowledgments**

31

32   **Abstract**

33   Cholera emergence is strongly linked to local environmental and ecological context. The 1991-

34   2004 pandemic emerged in Perú and spread north into Ecuador's El Oro province, making this a

35   key site for potential re-emergence. Machala, El Oro, is a port city of 250,000, near the Peruvian

36   border. Many livelihoods depend on the estuarine system, from fishing for subsistence and trade,

37   to domestic water use. In 2014, we conducted biweekly sampling for 10 months in five estuarine

38   locations, across a gradient of human use, and ranging from inland to ocean. We measured

39   water-specific environmental variables implicated in cholera growth and persistence: pH,

40   temperature, salinity, and algal concentration, and evaluated samples in 5 months for pathogenic

41   and non-pathogenic *Vibrio cholerae*, by polymerase chain reaction (PCR). We found

42   environmental persistence of pandemic strains O1 and O139, but no evidence for toxigenic

43   strains. Cholera presence was coupled to algal and salinity concentration, and sites exhibited

44   considerable seasonal and spatial heterogeneity. This study indicates that environmental

45   conditions in Machala are optimal for cholera re-emergence, with risk peaking during

46   September, and higher risk near urban periphery low-income communities. This highlights a

47   need for surveillance of this coupled cholera– estuarine system to anticipate potential future

48   cholera outbreaks.

49   **Introduction**

50   Cholera remains a severe global threat to public health and development efforts (WHO 2013).

51   According to the World Health Organization, the burden of cholera is at least 100 times greater

52   than current estimates (Zuckerman et al. 2007; WHO 2013), with 120,000 deaths and 3-5 million

53   cases each year worldwide. Previous studies suggest that outbreaks of cholera can be explained

54   by oceanographic variables (e.g., sea surface temperature, pH, salinity) and phytoplankton

55   blooms, indicating the potential to predict disease outbreaks (Jutla et al. 2010; Jutla et al. 2013).

56   A recent analysis of global cholera pandemics indicates that cholera outbreaks originate in

57   coastal regions, often during flood events, before spreading inland (Jutla et al. 2010). Our own

58   previous work suggests that both current and future coastal hotspots of cholera transmission are

59   far larger than current surveillance efforts can capture, with considerably higher potential

60   exposure than previously estimated (Escobar et al. 2015). Estuarine systems are a natural

61   intersection of coastal oceanographic conditions and human use; as productive systems for

62   fisheries, port locations for transport, and rich riparian soils, they are a highly exposed interface

63   for humans. Particularly because coastal estuarine systems often represent subsistence-level

64   dependence on the interface, in terms of artisanal fisheries, a higher likelihood of direct water

65   use, and simply greater physical exposure by proximity, it is also the most vulnerable of

66   populations that are most likely to be exposed to pathogens and the most flooding prone areas in

67   the world (Nicholls 1995; Dixon et al. 2006; De Sherbinin et al. 2007; Hanson et al. 2011;

68   Hallegatte et al. 2013; Cai et al. 2014).

69   The causative agent of human cholera, *Vibrio cholerae*, is thought to originate from

70   estuarine waters, based on phylogenetic information and its physiological requirements for

71   growth and persistence (Colwell and Huq 1994; Colwell 2004). *Vibrio cholerae* is endemic in

72   the Bay of Bengal (Bangladesh and India) and along coastal areas in Latin America (Lipp et al.

73   2002; Mutreja et al. 2011), and it persists environmentally in riverine, estuarine, and coastal

74   waters around the world (Lipp et al. 2002), Cholera epidemics have been found to follow

75   coastlines (Colwell 1996), and *V. cholerae* can be transmitted to humans via a wide range of

76   marine organisms, including zooplankton, aquatic plants, shellfish, and fish (Vezzulli et al.

77   2010).

78   Ecuador is a critical location to understand cholera and other climate and water-sensitive

79   diseases due to its (1) high potential for cholera outbreaks and the high incidence of other

80   climate-sensitive infectious diseases (e.g., leptospirosis, dengue), and (2) the strong influence of

81   oceanographic conditions on local climate and flooding during El Niño events (Rossel et al.

82   1996; Rossel and Cadier 2009; Hanson et al. 2011; Hallegatte et al. 2013; Cai et al. 2014).

83   Indeed, in January 1991, cholera re-emerged in Latin America after more than a century without

84   cases (Lacey 1995). In Ecuador, the 1991 cholera epidemic emerged in the south of the country

85   from a small fishing village in El Oro Province, and it is suspected that a fisherman introduced

86   the index case was traveling north from Perú (Dixon et al. 2006). From 1991 to 2004 over 90,000

87   cases of cholera were reported in Ecuador, with most cases from coastal provinces. El Oro and

88   Guayas provinces, located in southern coastal Ecuador, encompassed one of two disease

89   epicenters in the country. Recent studies suggest there is a high risk of a second epidemic in

90   Ecuador due to the presence of important risk factors including the growth of vulnerable urban

91   populations, decreased investment in cholera surveillance and prevention programs, increased

92   flood risk associated with climate change, and a street food culture that includes eating raw

93   shellfish (ceviche) (Malavade et al. 2011). In addition, Guayaquil (Guayas Province), the largest

94   city in Ecuador, has been identified as the third most vulnerable city in the world to future flood

95   risk (Hallegatte et al. 2013). Furthermore, it has been found that in populations with a high

96   prevalence of blood group O, such as in Latin America, illness from cholera is more severe, and

97   the requirements for rehydration and hospitalization of infected individuals are considerably

98   higher (Swerdlow et al. 1994; Nelson et al. 2009). Given these conditions, there is compelling

99   evidence that people in southern coast of Ecuador are a high-risk population and there is a

100   critical need for active cholera surveillance in this region.

101   To address this, we evaluated local variability in the presence of cholera in the estuarine

102   environment surrounding the city of Machala, El Oro province, a site identified as a current and

103   future coastal cholera hotspot (Escobar et al. 2015). We selected five sampling sites associated

104   with estuarine water access in Machala, Ecuador, representing a range of economic and human

105   activity conditions, in addition to different proximity to the ocean. Using water sampling

106   methodology, coupled with laboratory identification of *Vibrio cholerae* bacteria, we assessed the

107   local environmental and pathogenic conditions over a period of ten months. Strengthening

108   climate and water-sensitive infectious disease surveillance systems (WHO 2003; Zuckerman et

109   al. 2007) and further understanding of the role of environmental factors in disease outbreak and

110   transmission over time and space (Sedas 2007; Akanda et al. 2013) are urgently needed to target

111   cholera and other climate and water sensitive diseases.

112

113   **Methodology**

114   **Study Site**

115   Machala is a port city of approximately 250,000 inhabitants, with major economic activities

116   stemming from agriculture (bananas), aquaculture (shrimp farming), and fishing/shellfish

117   collection, both small-scale and semi-industrial scale. Five sampling sites were established

118 within the Machala estuarine system (Figure 1), selected for maximum heterogeneity, to include

119 highly built urban areas, ports, mangrove, and coastal sampling areas. The five sites were: Isla

120 Jambelí, Boca del Macho, Puerto Bolívar Boca, Puerto Bolívar Adentro, and Héroes de Jambelí.

121 Isla Jambelí site is on the outer edge of the coastal draining estuary, and the entrance to Jambelí

122 is interspersed with mangroves and shrimp farms. Boca del Macho is the open edge of the inner

123 estuary, in open water on shallow sand, with mangroves. Puerto Bolívar Boca is near the mouth

124 of the open harbor, characterized by heavy boat traffic, commercial fishing, and residences lining

125 the waterway, with mangroves and shrimp farming on the far side of the waterway. Puerto

126 Bolívar Adentro is further into the city, along the estuary, characterized by residential low-

127 income housing, with shrimp farms and mangroves across the Héroes waterway. Heroes de

128 Jambelí is the most inland site, characterized by low income and poor quality housing built along

129 mangroves at the edge of the city; outflow from the houses is visible directly into the water

130 (Figure 1). The port city of Machala is an important sentinel surveillance site, due to its location

131 along the Pan American highway, approximately 80km north of the Peruvian border, facilitating

132 significant movement of people and potential pathogens by land and sea.

133

134 **Water sampling**

135 At each of the five study sites (Figure 1), water sampling was conducted at high tide, twice

136 monthly along a transect with 3 sub-sites spaced 250 m apart, and 3 replicates per subsite. Three

137 1L surface water samples per subsite were collected in sterile polypropylene bottles, and placed

138 in coolers with ice for transport for the laboratory. For environmental sampling, using a YSI

139 water probe* (600 XLM V2 Sonde), we recorded Surface Temperature (ºC), Conductivity, pH,

140   Salinity, and Optic-T BGA PE (Phycoerythrin) [blue-green algae] (cells/ml, which we converted

141   to cells/µl for ease of visualization) at each end of the transect.

142

143   **Laboratory analyses**

144   Water samples were transferred to the laboratory in coolers for *Vibrio cholerae* testing and were

145   processed within 24 hours of collection. For laboratory analysis, a 1L water sample was filtered

146   through a Whatman membrane No. 1 and 0.22 µm membrane (Millipore) by vacuum. Then,

147   10mL of Phosphate Buffered Saline (PBS) (pH 7.4) was pipetted onto the retained contents on

148   the membrane and gently washed by pipette 15x. The PBS was left on the membrane to incubate

149   at room temperature for 15 minutes prior to collection in 50mL conical tube.

150

151   **DNA isolation and PCR**

152   Genomic DNA was extracted from bacterial pellet of the previous step with a QIAamp DNA

153   mini kit (Qiagen), following manufacture instructions. Diagnosis of cholera serogroups and the

154   detection of toxigenic genes were performed each by duplex PCR. Table 1 describes primers sets

155   used to amplify the *rfb* region of O1 and O139 serogroups and the toxin subunit A (ctxA) and

156   toxin coregulated pilus (tcpA) genes. For both duplex PCRs, master mix was as follows: 0.05

157   U/ul of JumpStart REDTaq DNA Polymerase (Sigma), 1X buffer, 0.2 mM dNTPs, 0.2 mM of

158   each primer set, 1 µl of template and ultrapure water to a final volume of 25 µl. The

159   amplification program for diagnosis of serogroups was adapted from Hoshino et al.(Hoshino et

160   al. 1998), using the following conditions: 5 minutes at 94°C, 35 cycles of 94°C for 1 minute,

161   55°C for 1 minute and 72°C for 1 minute and final extension of 72°C for 7 minutes. Positive

162   samples for either or both serogroups were subjected to toxigenic genes duplex PCR. The

163 amplification program was according to conditions described in Kumar et al.(Kumar et al. 2010):

164 3 minutes at 94°C, 30 cycles of 94°C for 30 seconds, 59°C for 30 seconds and 72°C for 1.2

165 minutes, and final extension of 72°C for 10 minutes. PCR products were resolved in a 2%

166 agarose gel and sequenced to verify gene amplification.

167

168 **Statistical analyses**

169 As the data were not normally distributed, we conducted non-parametric tests throughout. We

170 characterized the sampling sites for each environmental variable: Temperature, pH, Salinity, and

171 BGA, conducting Kruskal-Wallis rank sum tests on site means, and on monthly means. We then

172 examined whether *V. cholerae* prevalence at sites, and strain (i.e., O1, O139) prevalence

173 separately, was associated with environmental variables using a series of non-parametric

174 Kendall's tau correlations.

175

176 **Results**

177 **Environmental characteristics**

178 The probe recorded a range of 9-104 readings at each sub-site biweekly for 10 months. We

179 pooled all readings by month for analyses. Our sample sites differed significantly in

180 environmental characteristics (Figure 2), as shown by a series of Kruskal-Wallis rank sum tests

181 (Temperature: $\chi^2 = 206.19$, df = 4, $p < 0.0001$; Salinity: $\chi^2 = 2257.5$, df = 4, $p < 0.0001$; pH: $\chi^2 =$

182 1347.3, df = 4, $p < 0.0001$; BGA $\chi^2 = 1824.8$, df = 4, $p < 0.0001$). We found that Héroes de

183 Jambelí, the most inland site, had the highest BGA, and that Isla de Jambelí, the most coastal

184 site, had the highest salinity; while there were statistical differences between all sites in all the

185 environmental variables, there were no clear outliers in the other variables. Our sample sites

186   exhibited significant change in environmental characteristics across months (Figure 3), as shown

187   by a series of Kruskal-Wallis rank sum tests (Table 2). Temperature was lowest in August for all

188   sites – likely reflecting pacific upwelling, which cools the water, regardless of air temperature.

189   Salinity at the most inland site, Héroes de Jambelí, was consistently lowest, and showed the

190   smallest change across months, while the other sites had a decrease in salinity in May, then a rise

191   from July-December. Isla de Jambelí had the highest salinity, reflecting its location on the most

192   coastal site. BGA was highest at the most inland site, Héroes de Jambelí, peaking in May,

193   lagging temperature by a month. BGA shows the least temporal or spatial clustered pattern and

194   has no obvious seasonality across the year. Heroes de Jambeli, however, registered the highest

195   BGA values during the study (~25,000). pH appears to peak in December-January across all

196   sites, with a decrease in July-August; the coastal and inland sites showed low pH values across

197   seasons, while Boca del Macho registered consistently high pH values across months.

198

199   **Laboratory analyses**

200   Of a total of 405 individual water samples, collected between May – September, 382 were

201   diagnosed by PCR. We found 139 (36.4%) samples positive for *V. cholerae*, and 243 (64%)

202   negative. We found both O1 and O139 serogroups of *V. cholerae* present in the estuarine system

203   studied in Machala, Ecuador. Serogroup O139 was predominant; 118 (83.5%) samples were

204   O139, and 51 (35.3%) were O1 (30 samples contained both). We were able to detect *V.*

205   *cholerae* during each of the 5 months of sampling, nevertheless we found that prevalence

206   decreased drastically in July (Figure 4). By sequencing the samples, we confirmed that the PCR

207   protocol applied was proper for detection of *V. cholerae* serogroups O1 and O139 strains.

208

209   *Vibrio cholerae* **characteristics**

210   We pooled water samples within sites, to derive monthly *V. cholerae* prevalences across and

211   within sites (prevalence = positive/total samples tested). Overall monthly prevalence of *V.*

212   *cholerae* ranged from 0.3 (n=68) in July to 0.58 (n=45) in September, with site prevalence

213   ranging 0-1, with a mean monthly site prevalence of 0.35 (Figure 4A). Individual strain

214   prevalence was generally higher for O139 than O1, but we see that Puerto Bolívar Adentro and

215   Héroes de Jambelí were *V. cholerae* positive in every month and also had higher prevalences

216   than the other sites (Figure 4B and 4C). We found that the prevalence of *V. cholerae*, and O139

217   and O1 strains separately, were significantly associated with higher BGA (blue-green algae

218   densities), and that prevalence of *V. cholerae* the O1 strain were significantly associated with

219   lower salinity. We found no significant association between prevalence and temperature or pH

220   (Table 3).

221

222   **Discussion and Recommendations**

223   We found evidence of an environmental reservoir of *V. cholerae* in the estuarine waters of

224   Machala, Ecuador, in 2014. We confirmed the presence of *V. cholerae*, including pandemic

225   strains O1 and O139. We cannot rule out ongoing toxigenic presence, but we did not detect it in

226   our samples.

227   Our sites exhibited considerable seasonal and spatial heterogeneity in environmental

228   variables and *V. cholerae* prevalence, with clear peaks (and troughs) during specific months. For

229   example, we found peak *V. cholerae* prevalence in September, with highest values in two sites:

230   – Héroes de Jambelí and Puerto Bolívar Adentro (Figure 1), these sites are characterized by low

231   income housing on the edge of the city, while being inland sites, facing mangroves and shrimp

232   farms, and were found to have *V. cholerae* present in every month sampled. The lowest *V.*

233   *cholerae* prevalence was found in July, in which only the two most inland sites had *V. cholerae*

234   detection. Water temperature had the clearest temporal pattern, falling rapidly through July,

235   likely corresponding to Pacific upwelling, cooling the waters, and increasing nutrients in the

236   system (Strutton et al. 2001). We found that there was lowest salinity in the most inland site,

237   Héroes de Jambelí, and a higher concentration of BGA than in other sites. This is in contrast to

238   Isla Jambelí, a small island community furthest from the mainland and closest to the ocean, with

239   high salinity due to its coastal location; however, it did not have lower BGA than other sites.

240   We found that the timing of *V. cholerae* was coupled to the environmental variables we

241   measured. For example, water temperature, BGA, and pH decreased in most sites through

242   July/August, so did the overall prevalence of *V. cholerae*, but we only demonstrated significant

243   associations between prevalence and site and month specific levels of salinity and BGA. Average

244   ocean salinity is around 35 ppt, while freshwater rivers average around 0.5 ppt; clearly in this

245   estuarine system, we see a mixed or brackish system, ranging from the lower average of around

246   15 ppt at our most inland site, to a high approaching 34 ppt at our coastal site. We detected *V.*

247   *cholereae* at a range of salinities, finding a negative correlation with increasing salinity,

248   suggesting that the lower salinity may provide a more suitable environment for the growth of *V.*

249   *cholereae*, but that even the higher salinity approaching ocean concentrations do not prevent that

250   growth. This finding is consistent with previous work demonstrating the suitability of coastal

251   oceans for *V. cholereae*(Strutton et al. 2001), but reveals a finer scale relationship with salinity as

252   we move inland in an estuarine system, up the gradient to fresh water.

253   BGA (blue-green algae; a.k.a. cyanobacteria) are photosynthetic prokaryotes that can be

254   found in freshwater, marine, and terrestrial environments (Stanier and Bazine 1977). The

255   photosynthetic pigments of cyanobacteria include chlorophyll-*a* and the phycobiliprotein

256   phycoerythrin. Here we use BGA values to characterize water features and because BGA has

257   been associated with *V. cholereae* persistence (Epstein 1993). However, BGA itself also poses a

258   significant threat to humans through its production of cyanotoxins. BGA toxins include

259   neurotoxins, hepatotoxins, cytotoxins, irritants and gastrointestinal toxins (Codd et al. 2005).

260   Among these chemicals, microsystin, is a known liver carcinogen (Hunter 1998), and has been

261   detected in marine ecosystems (Miller et al. 2010). Exposure to these via skin contact, inhalation,

262   or ingestion, can result in a range of effects, from skin irritation and conjunctivitis, to kidney

263   damage and respiratory arrest (Codd et al. 1999). The World Health Organization (WHO)

264   recognizes BGA blooms as an emerging public health risk, and recommends the development of

265   early warning systems to detect scums (World Health Organization 1999; Falconer 2001;

266   Manganelli et al. 2012). We argue that BGA related diseases should be included in differential

267   diagnosis in Héroes de Jambelí, particularly during May, when a BGA increase was evident in

268   this study.

269   Temperature increase, coupled with high nutrient load, low flow, and thermal

270   stratification, generally results in increased growth rates of cyanobacteria, and its dominance in

271   the phytoplankton community (Davis et al. 2009; Elliott 2010; Huber et al. 2012). This could

272   explain the high BGA values early in the year (Figure 3). In addition, warm temperatures

273   promote increases in the number of days where BGA biomass exceeds thresholds established by

274   WHO (Davis et al. 2009; Elliott 2012). High temperature influences water column stability and

275   mixing depth, producing favorable conditions for BGA blooms (Robarts and Zohary 1987; Stal

276   et al. 2003). This association of temperature increase with BGA blooms is consistent across

277   coastal, estuarine, and inland waters (Paerl 1988). Thus, long term monitoring to measure BGA

278   biomass should be considered at least in Heroes de Jambeli and Puerto Bolivar -the sites report

279   the highest BGA values (Figure 2), particularly considering that a rise in water temperature is

280   associated with BGA emergence (Wasmund 1997; Kanoshina et al. 2003; Suikkanen et al. 2007),

281   increasing the risk of BGA diseases with imminent future climate warming.

282   In Ecuador, seawater eutrophication is a public health problem (World Health

283   Organization 1999).In fact, several species of BGA have been identified in aquatic environments

284   in Ecuador (Gunkel and Casallas 2002; Nedbalová and Sklenár 2008; Ramírez-Luna et al. 2008).

285   Unfortunately, while there is an increasing recognition of the negative health effects of BGA

286   blooms, monitoring in coastal marine waters is rare, and efforts are strongly biased to freshwater

287   systems (Nedbalová and Sklenár 2008), making our exploration in estuarine areas a crucial

288   update to the status of BGA in the country. This study was conducted in an average climate year,

289   providing a preliminary framework for monitoring coupled *V. cholerae* – estuarine dynamics for

290   potential emergence of cholera outbreaks in the region. This is particularly useful baseline

291   information for anticipating El Niño years, extreme climate events associated with warming

292   temperatures of surface ocean water and increased rainfall and flooding events. Climate change

293   projections indicate that the frequency of extreme El Niño events will increase in the future, (Cai

294   et al. 2014) increasing the risk of water-borne diseases endemic in the region, such as cholera,

295   typhoid, and leptospirosis, and provides valuable information to add *V. cholerae* in the public

296   health agenda to consider infectious diseases beyond the already important vector-borne

297   diseases, such as dengue fever, chikungunya, zika, and malaria.

298   Indeed, by May 2016, two years after the initiation of this study, the first case of cholera

299   was reported in Machala, after approximately 12 years with no case reports in Ecuador (2016).

300   An immuno-compromised individual was confirmed positive for *V. cholerae* serotype O1 non-

301 toxigenic, by the National Public Health Research Institute of the Ministry of Health. Our team

302 diagnosed the patient using the same PCR assay described here. Although the source of the

303 infection was not confirmed, this case report suggests a worrisome link to the results of our

304 epidemiological survey, and merits further examination.

305   This study highlights the urgency for active epidemiological surveys and the need for

306 public health interventions to reduce the risk of water-borne pathogens in vulnerable populations

307 from a holistic social-ecological perspective. The community Héroes de Jambelí is a low-income

308 peri-urban settlement with less than 50 families, established informally in 2002. The community

309 continues to lack adequate access to piped water, sewerage, and garbage collection due to their

310 status as an illegal settlement. Simple bamboo homes have built over the mangrove system, with

311 direct discharge of wastewater into the estuary. At the same time, this community's livelihood

312 depends on artisanal fisheries (e.g., crabs, mollusks) from these same estuaries. This vulnerable

313 coupled human-natural system results in high risk of emerging epidemics from water-borne

314 pathogens.

315   The results of this study, coupled with ongoing and previously published remote sensing

316 and GIS assessments, will allow us to identify geographic areas for future *V. cholerae*

317 surveillance across coastal Ecuador. In the future, we anticipate sampling additional sites where

318 we have identified geographic algal bloom hotspots, but which do not have historic reports of

319 cholera emergence – to serve as control sites for analyses, and to provide background levels of

320 *Vibrio* and other pathogens. This information will inform the development of predictive maps

321 and population attributable fractions to help translate surveillance and modeling data into

322 numbers that can inform policy development, identification of communities at increased risk of

323 cholera, and preventive interventions. Other future projects will include: continued development

324   of a training program in infectious disease surveillance, development of a web-based GIS

325   platform to integrate data sources and examine the role of environmental factors in *V. cholerae*

326   transmission over time and space, and development of an early warning system for climate-

327   sensitive diseases.

328 **References**

329 Akanda AS, Jutla AS, Gute DM, Sack RB, Alam M, Huq A, Colwell RR, Islam S (2013)

330   Population Vulnerability to Biannual Cholera Outbreaks and Associated Macro-Scale

331   Drivers in the Bengal Delta.

332 Cai W, Borlace S, Lengaigne M, Van Rensch P, Collins M, Vecchi G, Timmermann A, Santoso

333   A, McPhaden MJ, Wu L (2014) Increasing frequency of extreme El Niño events due to

334   greenhouse warming. Nat Clim Change 4:111–116.

335 Codd GA, Bell SG, Kaya K, Ward CJ, Beattie KA, Metcalf JS (1999) Cyanobacterial toxins,

336   exposure routes and human health. Eur J Phycol 34:405–415.

337 Codd GA, Morrison LF, Metcalf JS (2005) Cyanobacterial toxins: risk management for health

338   protection. Toxicol Appl Pharmacol 203:264–272.

339 Colwell RR (2004) Infectious disease and environment: cholera as a paradigm for waterborne

340   disease. Int Microbiol 7:285–289.

341 Colwell RR (1996) Global climate and infectious disease: the cholera paradigm. Science

342   274:2025.

343 Colwell RR, Huq A (1994) Environmental Reservoir of Vibrio cholerae The Causative Agent of

344   Choleraa. Ann N Y Acad Sci 740:44–54. doi: 10.1111/j.1749-6632.1994.tb19852.x

345 Davis TW, Berry DL, Boyer GL, Gobler CJ (2009) The effects of temperature and nutrients on

346   the growth and dynamics of toxic and non-toxic strains of Microcystis during

347   cyanobacteria blooms. Harmful Algae 8:715–725.

348   De Sherbinin A, Schiller A, Pulsipher A (2007) The vulnerability of global cities to climate

349   hazards. Environ Urban 19:39–64.

350   Dixon TH, Amelung F, Ferretti A, Novali F, Rocca F, Dokka R, Sella G, Kim S-W, Wdowinski

351   S, Whitman D (2006) Space geodesy: Subsidence and flooding in New Orleans. Nature

352   441:587–588.

353   Elliott A (2012) Predicting the impact of changing nutrient load and temperature on the

354   phytoplankton of England's largest lake, Windermere. Freshw Biol 57:400–413.

355   Elliott J (2010) The seasonal sensitivity of cyanobacteria and other phytoplankton to changes in

356   flushing rate and water temperature. Glob Change Biol 16:864–876.

357   Epstein PR (1993) Algal blooms in the spread and persistence of cholera. Biosystems 31:209–

358   221.

359   Escobar LE, Ryan SJ, Stewart-Ibarra AM, Finkelstein JL, King CA, Qiao H, Polhemus ME

360   (2015) A global map of suitability for coastal Vibrio cholerae under current and future

361   climate conditions. Acta Trop 149:202–211.

362   Falconer IR (2001) Toxic cyanobacterial bloom problems in Australian waters: risks and impacts

363   on human health. Phycologia 40:228–233.

364   Gunkel G, Casallas J (2002) Limnology of an equatorial high mountain lake—Lago San Pablo,

365   Ecuador: the significance of deep diurnal mixing for lake productivity. Limnol-Ecol

366   Manag Inland Waters 32:33–43.

367   Hallegatte S, Green C, Nicholls RJ, Corfee-Morlot J (2013) Future flood losses in major coastal

368   cities. Nat Clim Change 3:802–806.

369   Hanson S, Nicholls R, Ranger N, Hallegatte S, Corfee-Morlot J, Herweijer C, Chateau J (2011)

370   A global ranking of port cities with high exposure to climate extremes. Clim Change

371   104:89–111.

372   Hoshino K, Yamasaki S, Mukhopadhyay AK, Chakraborty S, Basu A, Bhattacharya SK, Nair

373   GB, Shimada T, Takeda Y (1998) Development and evaluation of a multiplex PCR assay

374   for rapid detection of toxigenic Vibrio cholerae O1 and O139. FEMS Immunol Med

375   Microbiol 20:201–207.

376   Huber V, Wagner C, Gerten D, Adrian R (2012) To bloom or not to bloom: contrasting

377   responses of cyanobacteria to recent heat waves explained by critical thresholds of abiotic

378   drivers. Oecologia 169:245–256.

379   Hunter P (1998) Cyanobacterial toxins and human health. J Appl Microbiol 84:35–40.

380   Jutla A, Akanda AS, Huq A, Faruque ASG, Colwell R, Islam S (2013) A water marker

381   monitored by satellites to predict seasonal endemic cholera. Remote Sens Lett 4:822–

382   831.

383   Jutla AS, Akanda AS, Islam S (2010) Tracking Cholera in Coastal Regions Using Satellite

384   Observations1. JAWRA J Am Water Resour Assoc 46:651–662.

385   Kanoshina I, Lips U, Leppänen J-M (2003) The influence of weather conditions (temperature

386   and wind) on cyanobacterial bloom development in the Gulf of Finland (Baltic Sea).

387   Harmful Algae 2:29–41.

388   Kumar P, Peter WA, Thomas S (2010) Rapid detection of virulence-associated genes in

389   environmental strains of Vibrio cholerae by multiplex PCR. Curr Microbiol 60:199–202.

390   Lacey SW (1995) Cholera: calamitous past, ominous future. Clin Infect Dis 20:1409–1419.

391   Lipp EK, Huq A, Colwell RR (2002) Effects of global climate on infectious disease: the cholera

392   model. Clin Microbiol Rev 15:757–770.

393   Malavade SS, Narvaez A, Mitra A, Ochoa T, Naik E, Sharma M, Galwankar S, Breglia MD,

394   Izurieta R (2011) Cholera in Ecuador: Current relevance of past lessons learnt. J Glob

395   Infect Dis 3:189.

396   Manganelli M, Scardala S, Stefanelli M, Palazzo F, Funari E, Vichi S, Buratti FM, Testai E

397   (2012) Emerging health issues of cyanobacterial blooms. Ann DellIstituto Super Sanità

398   48:415–428.

399   Miller MA, Kudela RM, Mekebri A, Crane D, Oates SC, Tinker MT, Staedler M, Miller WA,

400   Toy-Choutka S, Dominik C (2010) Evidence for a novel marine harmful algal bloom:

401   cyanotoxin (microcystin) transfer from land to sea otters. PLoS One 5:e12576.

402   Mutreja A, Kim DW, Thomson NR, Connor TR, Lee JH, Kariuki S, Croucher NJ, Choi SY,

403   Harris SR, Lebens M, others (2011) Evidence for several waves of global transmission in

404   the seventh cholera pandemic. Nature 477:462–465.

405   Nedbalová L, Sklenár P (2008) New records of snow algae from the Andes of Ecuador. Arnaldoa

406   15:17–20.

407   Nelson EJ, Harris JB, Morris JG, Calderwood SB, Camilli A (2009) Cholera transmission: the

408   host, pathogen and bacteriophage dynamic. Nat Rev Microbiol 7:10.1038/nrmicro2204.

409   doi: 10.1038/nrmicro2204

410   Nicholls RJ (1995) Coastal megacities and climate change. GeoJournal 37:369–379.

411   Paerl HW (1988) Nuisance phytoplankton blooms in coastal, estuarine, and inland waters.

412   Limnol Oceanogr 33:823–843.

413   Ramírez-Luna V, Navia AF, Rubio EA (2008) Food habits and feeding ecology of an estuarine

414   fish assemblage of northern Pacific Coast of Ecuador. Pan-Am J Aquat Sci 3:361–372.

415   Robarts RD, Zohary T (1987) Temperature effects on photosynthetic capacity, respiration, and

416   growth rates of bloom☐forming cyanobacteria. N Z J Mar Freshw Res 21:391–399.

417   Rossel F, Cadier E (2009) El Niño and prediction of anomalous monthly rainfalls in Ecuador.

418   Hydrol Process 23:3253–3260. doi: 10.1002/hyp.7401

419   Rossel F, Cadier E, Gómez G (1996) Las inundaciones en la zona costera ecuatoriana: causas ---

420   obras de protección existentes y previstas. l'Institut francais d'études Andines (IFE)

421   Sedas VTP (2007) Influence of environmental factors on the presence of Vibrio cholerae in the

422   marine environment: a climate link. J Infect Dev Ctries 1:224–241.

423   Stal LJ, Albertano P, Bergman B, von Bröckel K, Gallon JR, Hayes PK, Sivonen K, Walsby AE

424   (2003) BASIC: Baltic Sea cyanobacteria. An investigation of the structure and dynamics

425   of water blooms of cyanobacteria in the Baltic Sea—responses to a changing

426   environment. Cont Shelf Res 23:1695–1714.

427   Stanier R, Bazine G (1977) Phototrophic prokaryotes: the cyanobacteria. Annu Rev Microbiol

428   31:225–274.

429   Strutton PG, Ryan JP, Chavez FP (2001) Enhanced chlorophyll associated with tropical

430   instability waves in the equatorial Pacific. Geophys Res Lett 28:2005–2008.

431   Suikkanen S, Laamanen M, Huttunen M (2007) Long-term changes in summer phytoplankton

432   communities of the open northern Baltic Sea. Estuar Coast Shelf Sci 71:580–592.

433   Swerdlow DL, Mintz ED, Rodriguez M, Tejada E, Ocampo C, Espejo L, Barrett TJ, Petzelt J,

434   Bean NH, Seminario L (1994) Severe life-threatening cholera associated with blood

435   group 0 in peru: implications for the latin american epidemic. J Infect Dis 170:468–472.

436   Vezzulli L, Pruzzo C, Huq A, Colwell RR (2010) Environmental reservoirs of Vibrio cholerae

437   and their role in cholera. Environ Microbiol Rep 2:27–33.

438   Wasmund N (1997) Occurrence of cyanobacterial blooms in the Baltic Sea in relation to

439   environmental conditions. Int Rev Gesamten Hydrobiol Hydrogr 82:169–184.

440   WHO (2013) Cholera Annual Report. Wkly Epidemiol Rec 321–336.

441   WHO (2003) Cholera Unveiled: Global Task. Force on Cholera Control. World Health

442   Organization Geneva

443   World Health Organization (1999) Toxic Cyanobacteria in Water: A guide to their public health

444   consequences, monitoring and management.

445   Zuckerman JN, Rombo L, Fisch A (2007) The true burden and risk of cholera: implications for

446   prevention and control. Lancet Infect Dis 7:521–530.

447   (2016) Epidemiological Update: Cholera. 27 May, Washington, D.C.: PAHO/WHO; 2016. Pan

448   American Health Organization / World Health Organization., Washington, D.C.

449

450

451

452 **Table 1.** PCR primers set used in this study

Set	Primer	Sequence	Product	Reference
1	O1F2-1	GTT TCA CTG AAC AGA TGG G	192 bp	(Hoshino et al. 1998)
	O1R2-2	CGG TCA TCT GTA AGT ACA AC		Development and evaluation of a multiplex PCR assay for rapid
2	O139F2	AGC CTC TTT ATT ACG GGT GG	449bp	detection of toxigenic *Vibrio*
	O139R2	GTC AAA CCC GAT CGT AAA GG		*cholerae* O1 and O139
3	tcpA-F	ATG CAA TTA TTA AAA CAG CTT TTT AAG	675bp	(Kumar et al. 2010) Rapid Detection of Virulence-Associated Genes in Environmental
	tcpA-R	TTA GCT GTT ACC AAA TGC AAC AG		Strains of *Vibrio cholerae* by Multiplex PCR
4	ctxA-F	CGG GCA GAT TCT AGA CCT CCT G	564bp	(Singh et al. 2002)
	ctxA-R	CGA TGA TCT TGG AGC ATT CCC AC		Development of a hexaplex PCR assay for rapid detection of virulence and regulatory genes in *Vibrio cholerae* and *Vibrio mimicus*

453

454

455 **Table 2.** Kruskal-Wallis rank sum test results for each site and environmental variable

456 differences by month.

457

Environmental Variable	Site	X^2	DF	p-value
Temperature	Boca de Macho	832.65	9	0.0001
	Héroes de Jambelí	643.85	8	0.0001
	Isla de Jambelí	622.85	9	0.0001
	Puerto Bolívar Adentro	445.99	9	0.0001
	Puerto Bolívar Boca	625.44	9	0.0001
Salinity				
	Boca de Macho	837.16	9	0.0001
	Héroes de Jambelí	230.17	8	0.0001
	Isla de Jambelí	671.41	9	0.0001
	Puerto Bolívar Adentro	464.85	9	0.0001
	Puerto Bolívar Boca	619.21	9	0.0001
pH				
	Boca de Macho	534.3	9	0.0001
	Héroes de Jambelí	431.66	8	0.0001
	Isla de Jambelí	245.91	9	0.0001
	Puerto Bolívar Adentro	378.53	9	0.0001
	Puerto Bolívar Boca	416.76	9	0.0001
BGA				
	Boca de Macho	650.84	9	0.0001
	Héroes de Jambelí	309.2	8	0.0001
	Isla de Jambelí	469.75	9	0.0001
	Puerto Bolívar Adentro	219.78	9	0.0001
	Puerto Bolívar Boca	519.81	9	0.0001

458

459   **Table 3:** Kendall tau tests for correlation between prevalence of cholera, and each strain

460   separately, and environmental variables at sites, pooled monthly.

461

Environmental Variable	Prevalence	Kendall's τ	z	*p*-value
Temperature	*V. cholerae*	0.08	0.56	0.57
	O1	0.12	0.80	0.42
	O139	0.02	0.12	0.91
Salinity	*V. cholerae*	-0.34	-2.35	**0.02**
	O1	-0.35	-2.29	**0.02**
	O139	-0.28	-1.92	0.06
pH	*V. cholerae*	-0.10	-0.68	0.49
	O1	-0.14	-0.92	0.36
	O139	-0.10	-0.64	0.52
BGA	*V. cholerae*	0.55	3.76	**0.00**
	O1	0.48	3.09	**0.00**
	O139	0.49	3.34	**0.00**

462

463

464   **Figures**

465

466   **Figure 1:** Location of sampling sites. **A.** Ecuador (in yellow) in South America, indicating the

467   location of Machala (red point); **B.** Location of Machala on the southern coast of Ecuador (red

468   point); **C.** Location of the five sampling sites: Isla Jambelí, Boca del Macho, Puerto Bolívar

469   Boca, Puerto Bolívar Adentro, and Héroes de Jambeli (red points), in and around Machala

470   (green).

471

472   **Figure 2:** Environmental features in the study area. Water characteristics by site (means and

473   standard errors Temperature (TEMP, °C), Salinity (SAL), pH, and measured total concentration

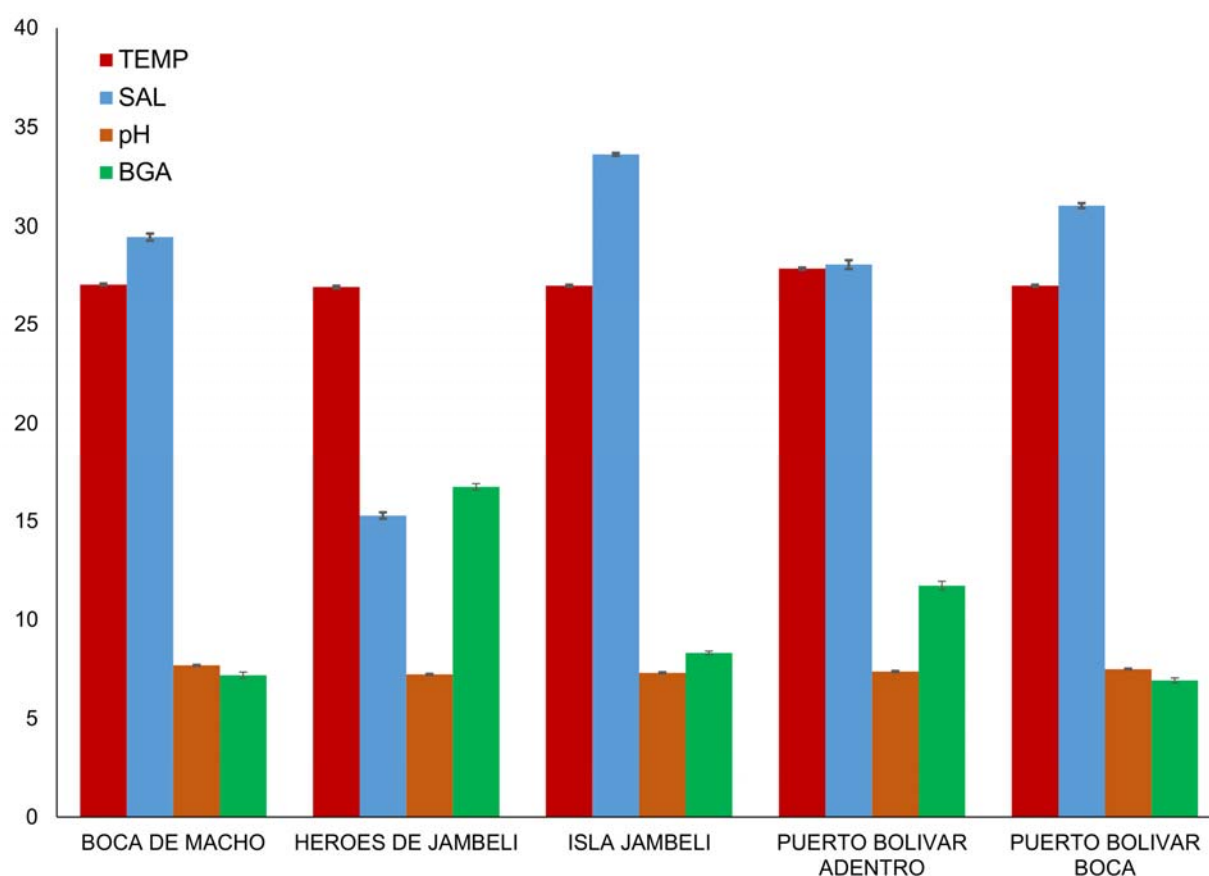474   of blue-green algae (BGA, cells/µL).

475

476   **Figure 3:** Environmental features in the study period. Water characteristics by month (means

477   and standard errors) and sites: **A**. Temperature (TEMP, °C), **B.** Salinity (SAL), **C.** measured total

478   concentration of blue-green algae (BGA, cells/µL), and **D.** pH.

479

480   **Figure 4:** *Vibrio cholerae* detection. Monthly site prevalence of **A.** cholera as given by positive
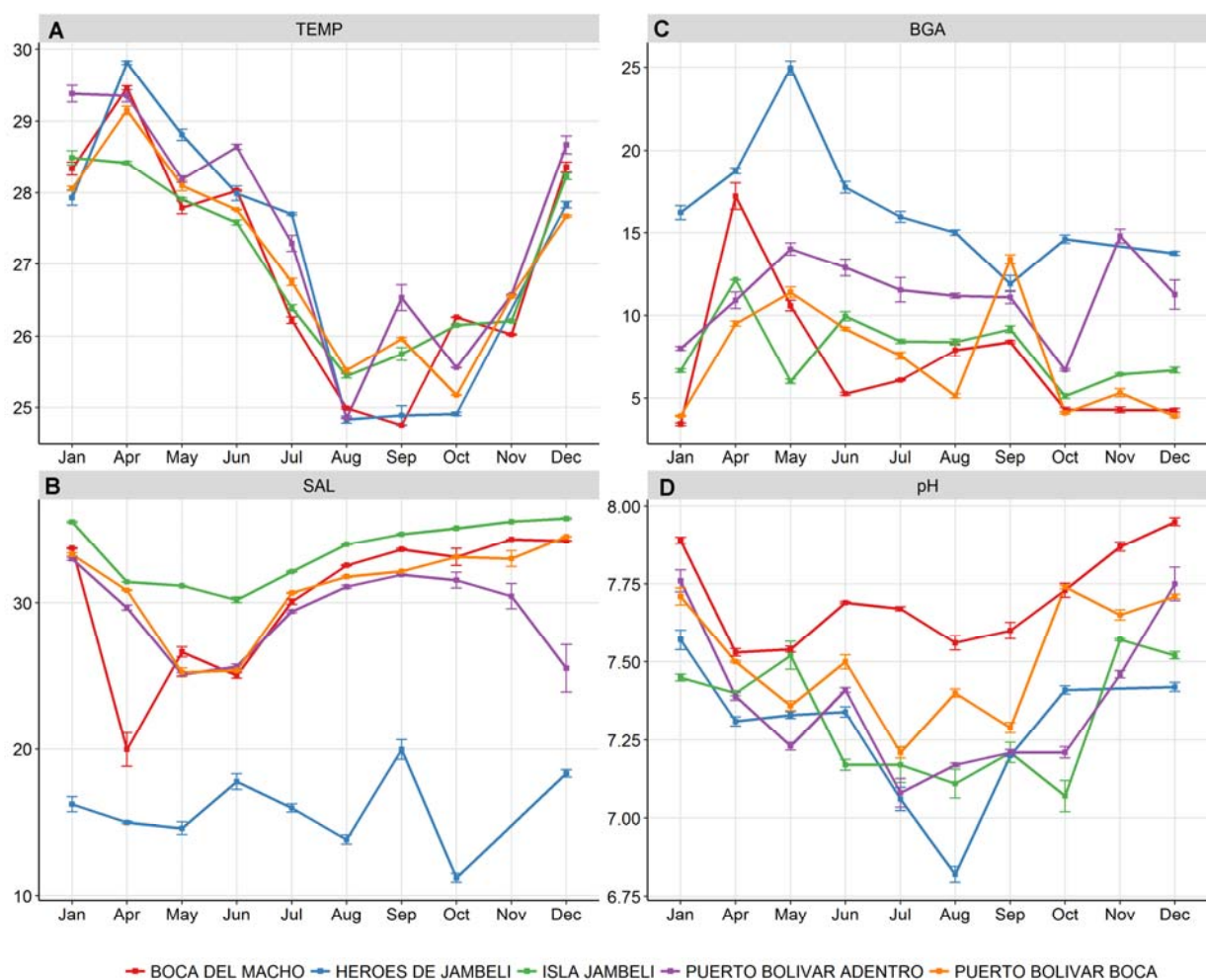
481   PCR test, **B.** O1 strain, **C.** O139 strain.

482
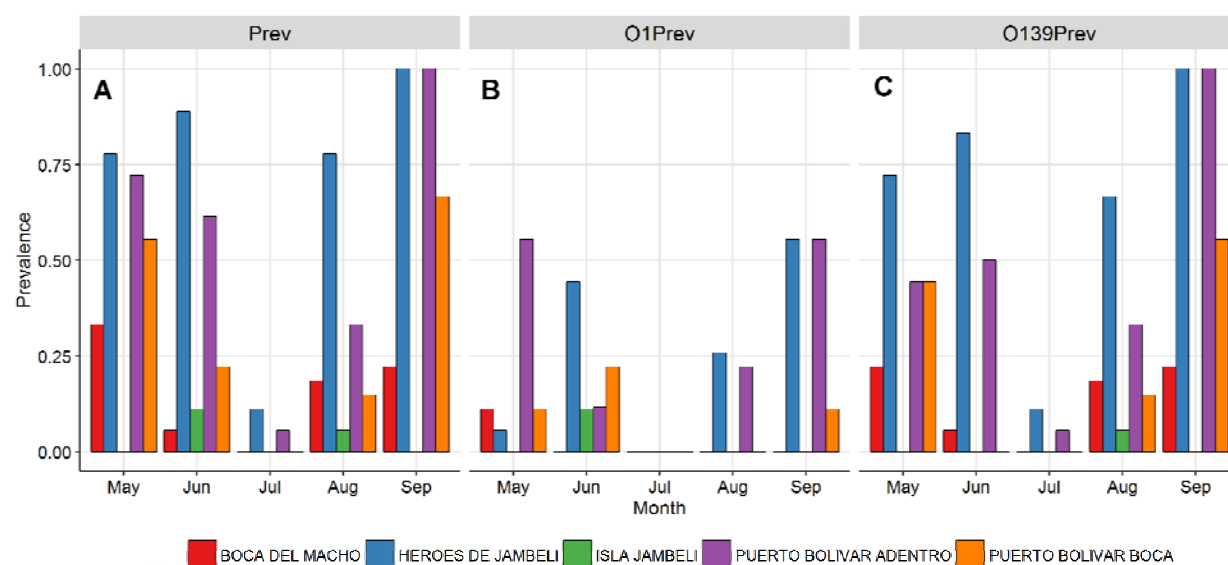
483 **Figure 1**

484

485

486   **Figure 2**

487

488

489

490   **Figure 3**

491

492

493　**Figure 4**

494